MECHANICAL BEHAVIOR OF SOIL-STEEL STRUCTURE SUBJECTED TO LIVE LOADS AND DIFFERENT WATER CONDITIONS[1]

Dariusz ŁYDŻBA*, Adrian RÓŻAŃSKI*, Maciej SOBÓTKA*,
Damian STEFANIUK* Grzegorz CHUDY**, Tomasz WRÓBLEWSKI**
*Wrocław University of Science and Technology, Faculty of Civil Engineering
** Hydroprojekt Wrocław Sp. z o. o.

The paper describes the analysis of a three-span soil-steel bridge along the road section crossing a dry anti-flood reservoir. The structure can be occasionally filled with water. The authors investigate internal forces and stresses in the shells due to live loads at different water conditions. Finite element simulations are carried out assuming elastic-plastic behavior of soil, elastic shell and nonlinear (frictional) contact zone. The analysis takes into account soil load history. In particular, the construction and operation of the bridge under quasi-static live loads is considered. The construction stage includes laying and compaction of the backfill. Then, the bridge in operation is investigated at three different water conditions: normal use (dry reservoir), maximum water level (flood) and lowering of the water level in the reservoir. The results show that during the flood the maximum stress in the shell significantly increases. Moreover, some of non-linear effects, typical in such structures, e.g. hysteretic effect, become more evident in comparison to normal use of the bridge.

1. INTRODUCTION

The soil-steel structures technology has been widely used in recent years to build bridges, culverts, tunnels, underpasses and passages for animals [1] [3] [13] [15] [16] [17] [21] [23]. The most beneficial advantages of this technology are, inter alia, relatively low costs [12] and short time of construction [11] as well as maintenance-free exploitation due to the lack of bridge bearings or expansion joints [19].

The mechanical behavior of such structures consists in the interaction between soil backfill and flexible shell [1] [9] [3] [7] [10] [14] [18] [20] [22]. As

a consequence the necessary volume of structural material can be significantly reduced compared to other technologies in the area of bridge engineering. However, the effect of soil-steel interaction entails further consequences [6]. The performance of such structures depends significantly on the quality of soil compaction and soil moisture. This is illustrated by the numerical analysis presented in the paper. The simulations reflect the behavior of soil-steel structure subjected to live loads under different water conditions.

2. THE BRIDGE UNDER CONSIDERATION

The soil-steel structure under analysis has been built in the vicinity of Roztoki village, Silesian region, Poland. A section of road No. 3233D with the bridge over Nowinka stream crosses dry anti-flood reservoir Roztoki Bystrzyckie (Fig. 1). The longitudinal cross-section of the bridge is presented in Fig. 2.
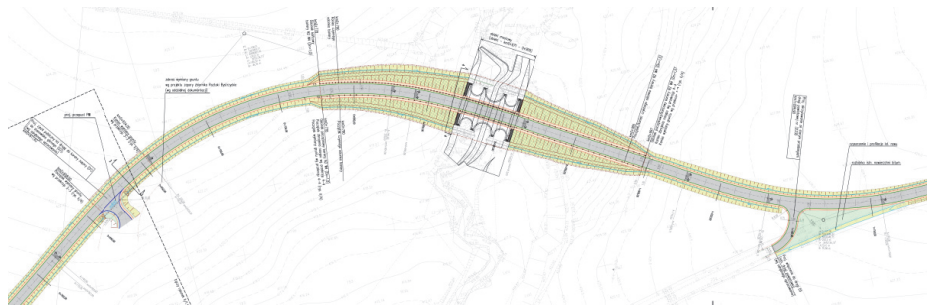

Fig. 1. Horizontal alignment of the road section with the bridge
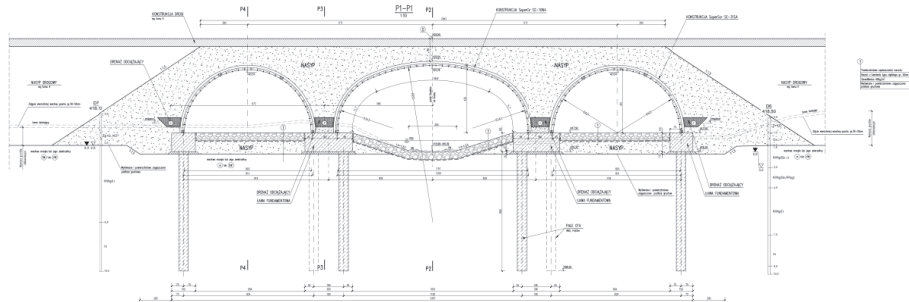

Fig. 2. Longitudinal cross-section of the bridge

The bridge is a three span soil-steel structure made of corrugated steel plates. The main span over the Nowinka stream is 12.0 m long, and the lateral ones are about 8.0 m in length and a play dual role: they are a passage for wild animals

and they enable free flow of water under the bridge during flood. The shells are supported on four continuous footings founded on CFA piles of 60 cm in diameter and 8.0 m in length. The steel structure is designed based on SuperCor system manufactured by ViaCon Polska Sp. z o.o. The central shell is denoted as SC-10NA whereas the lateral ones are of SC-31SA type [2]. All three shells are made of corrugated steel sheets 380x140x7 with the rib reinforcement covering the entire width. Soil backfill is made of properly compacted coarse sand. Slopes of the embankment are covered with natural stone set due to necessary protection against water inflow.

The road embankment as well as the culvert have been designed so that they could be accessible during the flood. During the design process, the following situations have been taken into account:

- normal use of the reservoir – no flood,
- increasing the water level – at the beginning of flood,
- maintaining the maximum water level,
- lowering the water level – transition to normal use after flood.

3. THE FRAMEWORK OF NUMERICAL SIMULATIONS

The plain strain analyses are carried out with the use of finite element software, ZSoil [8]. The elastic-plastic constitutive model with Coulomb-Mohr yield criterion is assumed for the backfill soil; the unassociated plastic flow rule is prescribed. The following material properties are used: Young modulus E=64.0 MPa, Poisson's ratio v=0.25, dry density ρ_d=1.9 t/m^3, internal friction angle ϕ=28° and dilation angle ψ=0.1·ϕ. In order to ensure numerical stability of simulation, a non-zero value of cohesion is assumed, namely c=1.0 kPa.

Utilizing the Richard's hypothesis [25] on the continuity of gas phase in vadose zone, a saturation degree above the water table is evaluated with respect to van Genuchten model [24]:

$$s(h) = s_r + \frac{s_s - s_r}{\left(1 + \left(1 - \mathrm{H}(h)\right) \cdot \left(\alpha \cdot |h|\right)^m\right)^{\left(1 - \frac{1}{m}\right)}}, \tag{1}$$

where (the values used in simulations are provided in the brackets):
s_r – residual saturation ratio (s_r=0),
s_s – degree of saturation in the saturated zone (s_s=1),
α, m – model parameters (α=2 [m^{-1}] and m=2),
h – hydraulic head,
$\mathrm{H}(h)$ – Heaviside's function.

The water flow through the backfill soil is governed by the generalized Darcy's law [8]:

$$\vec{q} = -k \cdot \hat{k}(s) \cdot \text{grad}(h+z), \tag{2}$$

In the equation above:

$\vec{q}$ – is the flux (discharge per unit area),

k – is the permeability coefficient ($k=1*10^{-3}$ m/s),

$\hat{k}(s) = s^3$ – is the coefficient taking into account the saturation degree of the backfill soil,

z – stands for the vertical coordinate.

The corrugated shell is modeled with the use of beam elements. A linear-elastic constitutive model is assumed. Material properties, used in the calculations, are as follows: Young's modulus E_S=205.0 GPa and density ρ_d=7.86 t/m^3. The steel shell is connected with the foundation by pinned support. The interface is generated between the backfill soil and the corrugated shell. The one-sided contact interface is defined, i.e. separation is allowed. The value of shear stress, in contact elements, is governed by the Coulomb condition:

$$\left| \tau_f \right| \le a + \sigma \, \text{tg} \, \delta . \tag{3}$$

Adhesion and the friction angle between soil and steel is assumed as a=0 kPa and δ=0.5·ϕ, respectively. In the saturated zone the value of δ is reduced to the value δ_s=1.0°. Zero value of the dilation angle in contact elements is assumed. Both normal and tangential interface stiffness are adopted in accordance with the ZSoil user manual [8].

In the numerical simulations three stages are considered, i.e. stage I – laying and compaction of the backfill, stage II – bridge in operation and no water in the reservoir, stage III – continued use of the bridge at different scenarios concerning water levels in the reservoir. In stage I the overall soil load history is taken into account. In particular, backfilling with successive soil layers of 0.5 m thicknesses is included – it is numerically modeled by prescribing to the successive layers the double bounded uniformly distributed load of intensity q=50.0 kPa. The load sequence for a chosen layer is presented in Fig. 3.

Stage II corresponds to the normal use of the bridge and it is a continuation of modeling carried out in stage I. A quasi-static live load K and q of class C, in accordance with Polish standard PN-85/S-10030 [5], is included in the simulations. Design loads are calculated by applying load factor γ_f=1.5. The movement of load K is performed as a sequence of consecutive load positions. Each time the load is moved to the new position, the boundary value problem is solved once again. The location of load K is defined by variable X, standing for a distance between symmetry axis of the load and symmetry axis of the bridge. In particular, X=0 means that the load is positioned in the centre of the bridge (see Figs. 4–6). The movement of the load between extreme positions (X=-26.0m; X=+26.0 m) is performed by 270 successive locations. In this stage two load

cycles are performed; the load cycle means the movement of load K between extreme positions from the starting position to the other side and then back.
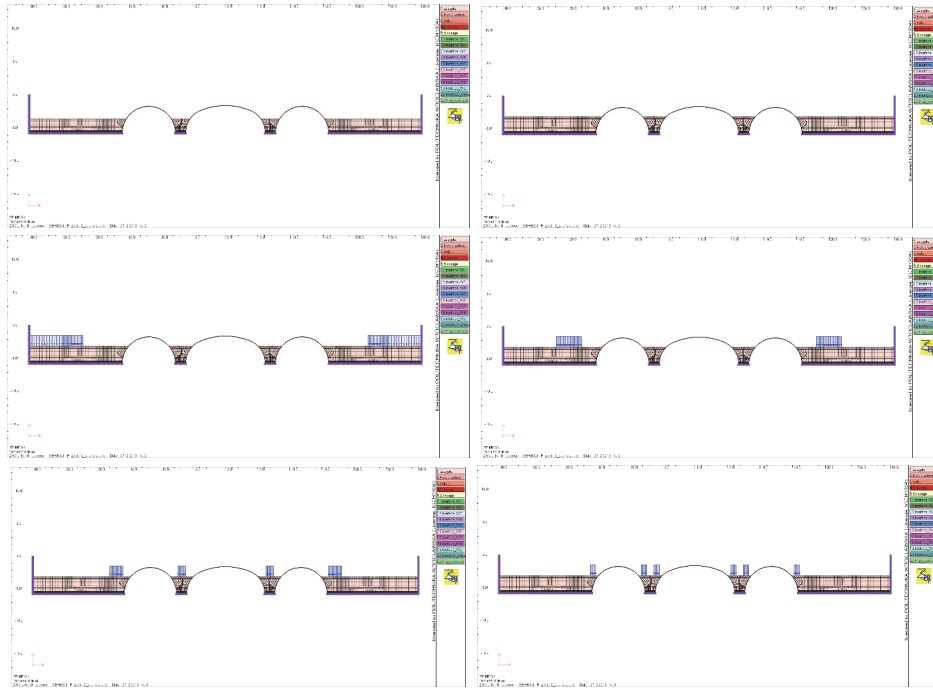

Fig 3. Load applied on a third layer at stage I (laying and compaction of the backfill)

In the next part of simulations (stage III), additional two load cycles are considered for different water conditions, namely:

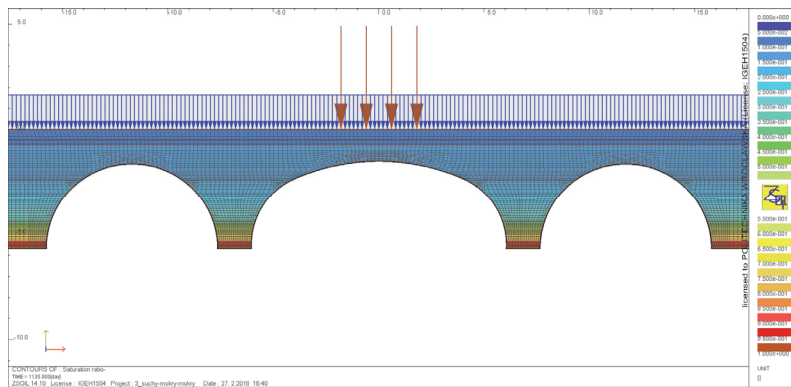− **scenario I**: continued normal use of the bridge, no water in the reservoir (Fig. 4).

Fig. 4. Degree of saturation of backfill soil and applied loads: stage III/scenario I

− **scenario II**: continued use of the bridge, maximum water level in the reservoir (backfill soil is fully saturated up to 421.70 m a.s.l.) – Fig. 5.
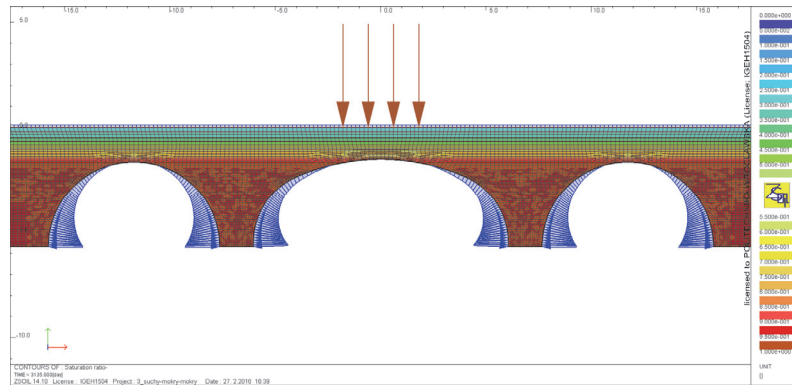

Fig. 5. Degree of saturation of backfill soil and applied loads: stage III/scenario II

− **scenario III**: it is a continuity of scenario II; in addition, lowering of the water level in the reservoir is considered; thus, the backfill soil is still saturated up to 421.70 m a.s.l.; however there is no hydrostatic water pressure applied to the external side of the shells (Fig. 6).
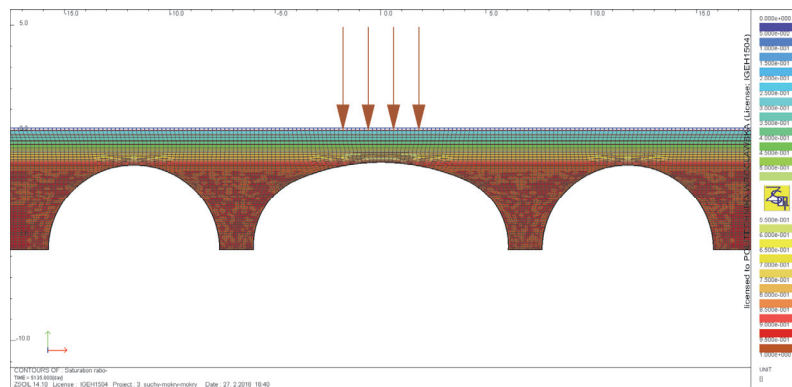

Fig. 6. Degree of saturation of backfill soil and applied loads: stage III/scenario III

4. RESULTS OF NUMERICAL CALCULATIONS

When the sequence of boundary value problems is solved, the displacement fields in the backfill soil and steel shells are determined. Since the main aim of this paper is to investigate the influence of different water conditions on the state of stress in steel shells, we mention very briefly the results obtained at stage I, in

which the construction of the bridge is considered. Results for stage II are not presented in the paper. In Fig. 7 the deformed shells at stage I are shown. We can observe different behavior of central and lateral shells. In the case of the former one, the displacement of crown is downward, whereas the side walls displacement is in the direction of the ground (outward). The two remaining shells exhibit the opposite behavior. This is mainly triggered by different geometry of central (box structure) and lateral shells (arched structure) as well as by the interaction between neighboring shells of different type.
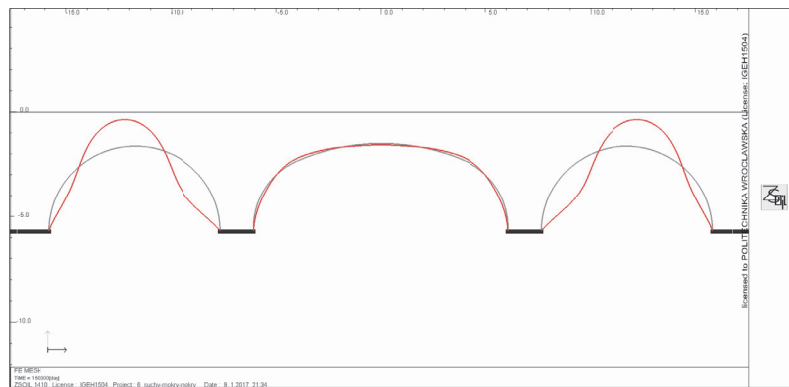

Fig. 7. Deflection of the shells – stage I (construction of the bridge)

As mentioned before, the results obtained in stage I and II are not discussed here, however, they are the "input" – in the sense of soil load history – to the numerical calculations performed in stage III. For the purpose of the analyses of the influence of different water conditions on the state of stress in steel shells, first the distributions of internal forces (bending moment M_z and axial force N_x) in beam elements were evaluated. Based on the values of internal forces, the maximum values of normal stress in shells were calculated with respect to the following relation:

$$\sigma_x = \frac{|N_x|}{A_x} + \frac{|M_z|}{W_z},$$ (4)

where A_x and W_z are geometrical characteristics, i.e. cross sectional area and section modulus, respectively. Four points located in the top part (1 and 4) and side walls (2 and 3) of shells were chosen for the considerations; in these points the maximum values of normal stress were observed. The location of these points is presented in Fig. 8.
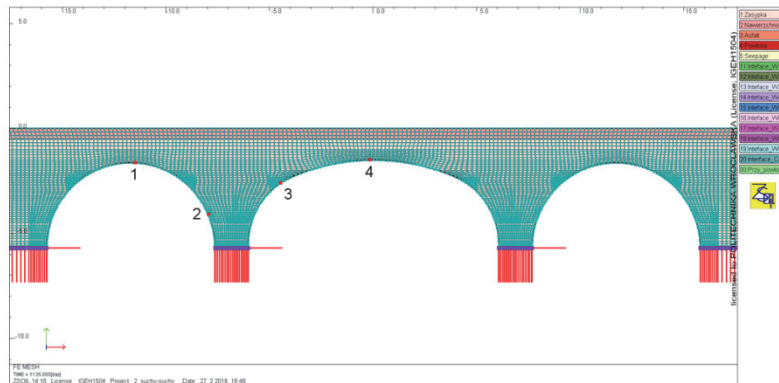
Fig. 8. Location of characteristic points

4.1. Stage III – scenario I

The results obtained for this scenario correspond to the situation of no water in the reservoir (normal use of the bridge – see Fig. 4). Fig. 9 presents charts of normal stress σ_x versus load position X in characteristic points 1–4.
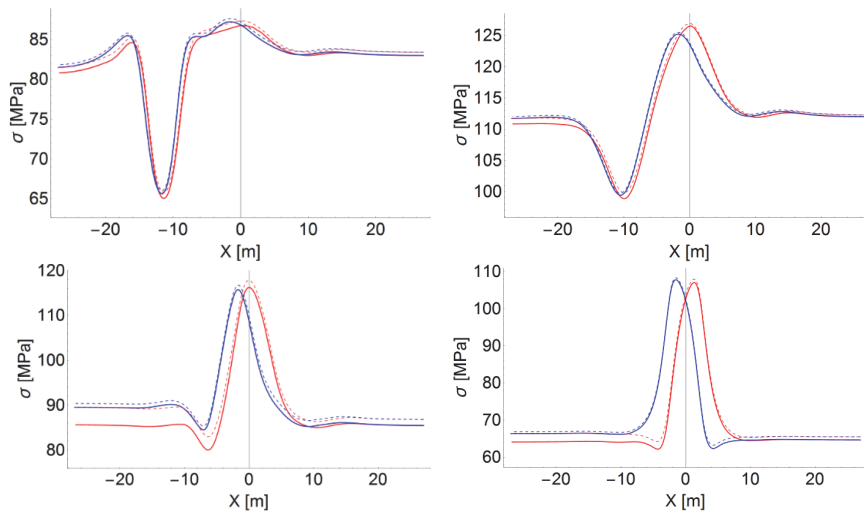

Fig. 9. Plots of normal stress σ_x versus load position X in characteristic points for scenario I: top left – 1, top right – 2, bottom left – 3 and bottom right – 4

The arrangement of the graphs is as follows: top left and top right plots present the results for the side shell (points 1 and 2, respectively) whereas bottom left and bottom right plots show the distribution of σ_x for middle shell (points 3 and 4, respectively) Moreover, the continuous lines correspond to the results obtained for the first load cycle; dashed lines – the second load cycle. Red and

blue colors represent the movement of the load to the right (from *x*=-26.0 m to *x*=+26.0 m) and to the left (from *x*=+26.0 m to *x*=-26.0 m), respectively.

4.2. Stage III – scenario II

As mentioned earlier the results obtained for this scenario correspond to the use of the bridge during the flood (backfill soil is fully saturated up to 421.70 m a.s.l., Fig. 5). The distribution of normal stress with respect to the localization of load *K* is shown in Fig. 10. Note that the results are presented in the same manner as for scenario I.

Fig. 10. Plots of normal stress σ_x versus load position *X* in characteristic points for scenario II: top left – 1, top right – 2, bottom left – 3 and bottom right – 4

4.3. Stage III – scenario III

As mentioned earlier scenario III is a continuity, in the sense of numerical simulations, of the analyses performed for scenario II. The results presented here concern the situation of lowering of the water level in the reservoir – the backfill soil is still saturated up to 421.70 m a.s.l., however there is no hydrostatic water pressure applied to the shells (Fig. 6). In Fig. 11 normal stress plots for all characteristic points are presented.
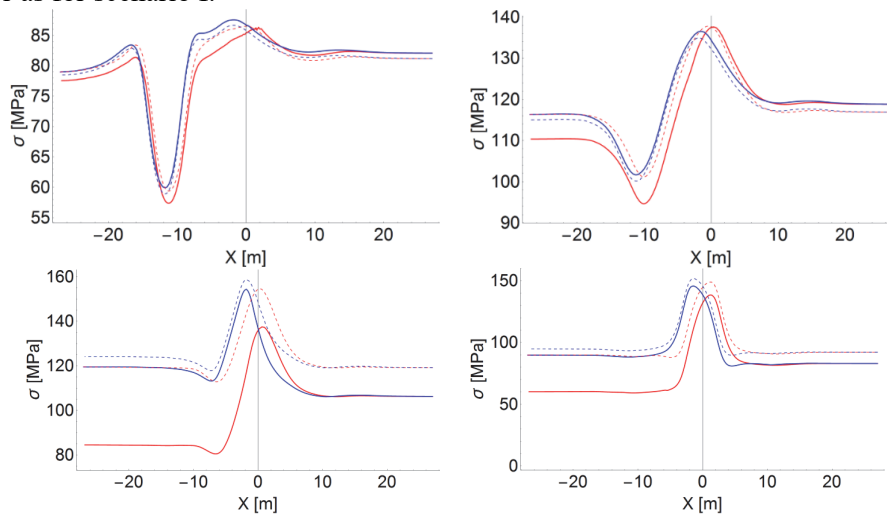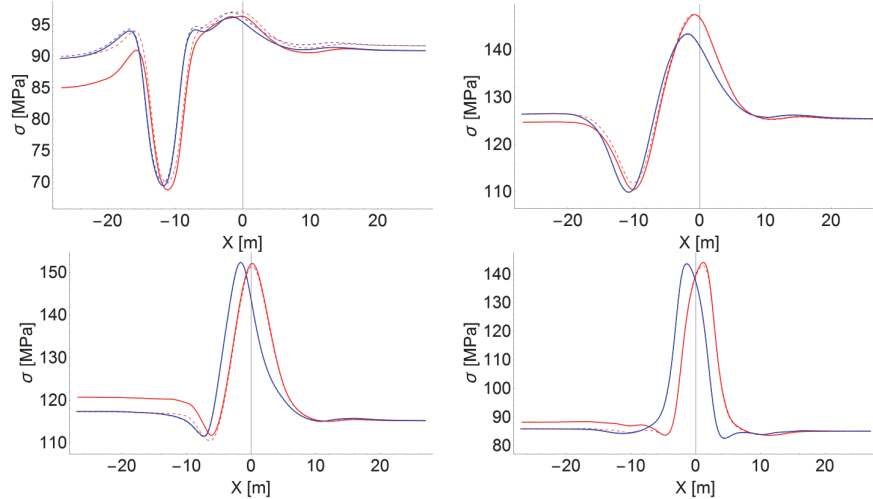
Fig. 11. Plots of normal stress σ_x versus load position X in characteristic points for scenario III: top left – 1, top right – 2, bottom left – 3 and bottom right – 4

5. DISCUSSION OF RESULTS AND CONCLUSIONS

The numerical simulations presented in the paper indicate that the behavior of soil steel-structures depends on phreatic surface location within soil backfill as well as the soil compaction at the construction stage. Based on the obtained results, presented in the previous section, it can be concluded that for all scenarios:

- stress plots for all characteristic points exhibit the so called hysteretic effect, i.e. plot lines corresponding to the particular (opposite) directions of load movement do not overlap,
- the effect of non-zero residual stress, remaining in the structure after consecutive load cycles, is clearly visible.

The above-mentioned features are typical for soil-steel flexible structures [3] [4] [6] [7]. Furthermore, the simulation of the structure during the flood (scenarios II and III) indicates that the stress level generally increases compared to normal use of the bridge (scenario I). Thus, the full saturation of the backfill soil is unfavorable for the structure. The values of maximum stress for all characteristic points are summarized in Table 1.

Table 1. Extreme values of stress σ_x

Scenario	Stress σ_x [MPa] in reference points:			
	1	2	3	4
I	87.60	126.9	117.8	108.3
II	87.57	137.8	158.7	151.6
III	97.10	147.5	152.4	144.1

As it can be easily noticed, the maximum stress value increases by about 20–25% during the flood (scenarios II and III) compared to the normal use of the bridge (scenario I). Furthermore, the results obtained in the simulation of flood show more evident hysteretic effect – the shift in plots of σ_x for opposite directions is more evident. In particular, scenario III is recognized as the most unfavorable one for lateral shells. In the case of central shell the opposite situation is observed, i.e. the most unfavorable is scenario II. It is due to the fact that the deflection state induced in stage I (laying and compaction of the backfill) influences the behavior of the structure at successive stages. After stage I, the lateral shells deflect so that the crown moves upwards while the sides displace inwards. In the case of central shell the situation is roughly opposite. Thus, the water pressure applied to the external side of shells at stage II implies the increase in stress in the case of central shell and decrease in the lateral ones.

LITERATURE

[1] Janusz L., Madaj A., *Obiekty inżynierskie z blach falistych: projektowanie i wykonawstwo*. Wydawnictwo Komunikacji i Łączności, 2009.

[2] Katalog: *Konstrukcje podatne z blachy falistej SuperCor*. ViaCon. Ed. 01/2013.

[3] Machelski, C., *Modelowanie mostowych konstrukcji gruntowo-powłokowych*. Dolnośląskie Wydawnictwo Edukacyjne, 2008.

[4] Machelski C., Antoniszyn G., Michalski B., "Live load effects on a soil-steel bridge founded on elastic supports." *Studia Geotechnica et Mechanica* 28, 2-4 (2006): 65-82.

[5] PN-85/S-10030 *Obiekty mostowe. Obciążenia.*

[6] Sobótka, M., *Wieloskalowe modelowanie numeryczne współpracy zasypki z powłoką w konstrukcjach gruntowo-powłokowych*, Praca doktorska. Politechnika Wrocławska 2016.

[7] Sobótka M., "Numerical simulation of hysteretic live load effect in a soil-steel bridge." *Studia Geotechnica et Mechanica* 36.1 (2014): 103–109.

[8] *ZSoil manual*, Elmepress and Zace Services Limited, Lausanne, Switzerland, 2014.

[9] Bayoglu Flener E., Sandquist H., "Field testing of a long-span arch corrugated-steel culvert under dynamic and static loads." *Archiwum Instytutu Inżynierii Lądowej/Politechnika Poznańska*. 1 (2007): 25-33.

[10] Bayoglu Flener E., Sandquist H., "Full-scale testing of two corrugated steel box culverts with different crown stiffness." *Archiwum Instytutu Inżynierii Lądowej/Politechnika Poznańska* 1 (2007): 35-44.

[11] Bednarek B., Czerepak A., "Animal crossing built over A2 motorway in Poland." *Archiwum Instytutu Inżynierii Lądowej/Politechnika Poznańska* 1 (2007): 45-51.

[12] El-Sawy K.M., "Three-dimensional modeling of soil-steel culverts under the effect of truckloads." *Thin-walled structures* 41.8 (2003): 747-768.

[13] Korusiewicz L., Kunecki B., "Field test of a large-span soil-steel arch without stiffeners during backfilling operations." *Archiwum Instytutu Inżynierii Lądowej/Politechnika Poznańska* 12 (2012): 133-139.

[14] Kunecki B., "Full-scale test of corrugated steel culvert and FEM analysis with various static systems." *Studia geotechnica et mechanica* 28.2-4 (2006): 5-19.

[15] Kunecki B., *Zachowanie się ortotropowych powłok walcowych w ośrodku gruntowym pod statycznym i dynamicznym obciążeniem zewnętrznym.* Praca doktorska, Politechnika Wrocławska, 2006.

[16] Kunecki B., Korusiewicz L., "Field Test of Soil-Steel Corrugated Arch with Ribs and Three-Dimensional Analysis." *Transportation Research Board 91st Annual Meeting.* 12-1507. (2012).

[17] Kunecki B., Vaslestad J., Janusz L., "Przykłady kształtowania przestrzeni komunikacyjnej z zastosowaniem konstrukcji podatnych–doświadczenia z Polski i Norwegii." *Czasopismo Techniczne. Architektura* 104.4-A (2007)

[18] Machelski C., Marcinowski J., "Numerical modelling of moving load effect in a soil-steel bridge." *Archiwum Instytutu Inżynierii Lądowej/Politechnika Poznańska* 1(2007): 155-165

[19] Mattsson H-Å., Sundquist H., "The real service life and repair methods of steel pipe culverts in Sweden." *Archiwum Instytutu Inżynierii Lądowej/Politechnika Poznańska* (2007): 185-193.

[20] Michalski J.B., Michalski B., "Charakterystyczne cechy sprężenia w obiektach gruntowo-powłokowych." *Archiwum Instytutu Inżynierii Lądowej/Politechnika Poznańska* 8 (2010): 215-244.

[21] Pettersson L., Leander J., Hansing L., "Fatigue design of soil steel composite bridges." *Archiwum Instytutu Inżynierii Lądowej/Politechnika Poznańska* 12 (2012): 237-242.

[22] Sobótka M., Łydżba D., "Shape Optimization of Soil-Steel Structure by Simulated Annealing." *Procedia Engineering* 91 (2014): 304-309.

[23] Tomala P., Markowicz K., Bresch B., "Elements of the design process of the flexible steel arch over double track electrified railway." *Archiwum Instytutu Inżynierii Lądowej/Politechnika Poznańska* 1 (2007): 225-232.

[24] van Genuchten, M.T. (1980), *A closed-form equation for predicting hydraulic conductivity of unsaturated soils*, Soil Science Society of America Journal, 44(5): pp. 892-898.

[25] Richard, L.A. (1931), *Capillary conduction of liquids through porous mediums*, Journal of Applied Physics, 1: pp. 318-333.